



Flexible dynamic vine copula models for multivariate time series data[☆]



Elif F. Acar^{a,d,e,*}, Claudia Czado^b, Martin Lysy^c

^a Department of Statistics, University of Manitoba, Canada

^b Lehrstuhl für Mathematische Statistik, Technische Universität München, Germany

^c Department of Statistics and Actuarial Science, University of Waterloo, Canada

^d The Hospital for Sick Children, Canada

^e Department of Statistical Sciences, University of Toronto, Canada

ARTICLE INFO

Article history:

Received 12 July 2018

Revised 9 March 2019

Accepted 9 March 2019

Available online 30 March 2019

MSC:

00-01

99-00

Keywords:

Dynamic vines

Exchange rate dependence

Kendall's tau

Local likelihood

Multivariate time series

ABSTRACT

The representation of temporal patterns is essential to time series analysis. In the case of two or more time series, one needs to account for temporal patterns not only in each univariate series but also in their joint behavior. A multivariate model is proposed here for the specification of time-varying dependence patterns in multivariate time series in a flexible way. The model is built by first addressing the temporal patterns in each series and then modeling the interdependencies among their innovations using a time-varying vine copula model. To specify the vine decomposition, a heuristic model selection tool that accounts for both the magnitude and variation of the empirical Kendall tau across different time intervals is employed. The time variation in the strength of pairwise dependencies is inferred using nonparametric smoothing techniques, and the uncertainty in the resulting estimates is assessed using a parametric bootstrap. The methods are evaluated in a simulation study and used to analyze daily exchange rate returns of seven major currencies from August 2005 to August 2016.

© 2019 EcoSta Econometrics and Statistics. Published by Elsevier B.V. All rights reserved.

1. Introduction

Most applications of economics and finance involve multivariate time series data where a number of different quantities are simultaneously recorded over a period of time. Of interest in such settings is to understand the dependence among the quantities in addition to the temporal patterns in each univariate series. For instance, individual screening of exchange rate fluctuations is important to determine macroeconomic indicators at the country level, but offers only limited insight for risk management in a global economy. On the other hand, a broad understanding of co-movements in the foreign exchange rate market is critical for investors and policy makers to strategize their decisions.

There exists a multitude of econometric models to account for temporal patterns in time series data. The class of generalized autoregressive conditional heteroscedasticity (GARCH) models (Bollerslev, 1986; Engle and Bollerslev, 1986) is a popular choice due to its success in removing volatility clustering, which is present in most financial data. To date, several extensions of GARCH models to multivariate settings have been proposed (see Bauwens et al., 2006, for a survey). While the early work has focused on modeling the conditional variances and covariances assuming that the conditional correlations remain

[☆] Declarations of interest: none

* Corresponding author at: Department of Statistics, University of Manitoba, Canada.

E-mail address: elif.acar@umanitoba.ca (E.F. Acar).

constant (Bollerslev, 1990), considerable research efforts have since been directed at modeling time-varying dependence patterns in multivariate time series. Noting that temporal patterns may persist on the conditional correlations, Tse and Tsui (2002) and Engle (2002) proposed the dynamic conditional correlation (DCC)-GARCH model. Addressing evident asymmetric dependencies in multivariate financial data, Patton (2006) relaxed the distributional assumptions of the conventional multivariate GARCH models via time-varying (conditional) copulas. The latter approach, broadly referred to as copula-GARCH, has gained significant popularity in multivariate time series analysis, resulting in several applied works and methodological developments (e.g., Van den Goorbergh et al., 2005; Jondeau and Rockinger, 2006; Chen and Fan, 2006).

Copulas are multivariate distribution functions with uniform margins. They allow the interdependence among multivariate time series innovations to be flexibly captured, upon filtering these from the temporal patterns in each univariate series. In many practical settings with financial data, a common choice is to use a GARCH(1,1) model for each univariate series $R_{i,t}$.

$$R_{i,t} = \mu_i + \varepsilon_{i,t}, \quad \varepsilon_{i,t} = \sigma_{i,t} Z_{i,t}, \quad \sigma_{i,t}^2 = \omega_i + \alpha_i \varepsilon_{i,t-1}^2 + \beta_i \sigma_{i,t-1}^2, \quad (1)$$

where $i = 1, \dots, d$ and $t = 1, \dots, T$. The interdependence among the multivariate series is then characterized by the joint distribution F_t of the standardized innovations $Z_{1,t}, Z_{2,t}, \dots, Z_{d,t}$, which has a copula representation (Sklar, 1959),

$$F_t(Z_{1,t}, \dots, Z_{d,t}) = C_t\{F_1(Z_{1,t}), \dots, F_d(Z_{d,t})\}, \quad (2)$$

where F_i is the marginal distribution of $Z_{i,t}$, for $i = 1, \dots, d$ and C_t is the copula of $Z_{1,t}, Z_{2,t}, \dots, Z_{d,t}$. These models have been extensively studied in the bivariate case ($d = 2$) assuming time-invariant dependence $C_t \equiv C$: see, for instance, Cherubini et al. (2004), McNeil et al. (2005) and the references in the survey by Patton (2012). A more general treatment of copula models can be found in the monographs of Nelsen (2006) and Joe (1997, 2014).

Pioneered by Patton (2006), research efforts to incorporate time-varying dependence in copula models predominantly focus on parametric specifications. In these approaches, while the copula family is assumed to be time-invariant, its (suitably transformed) dependence parameter is considered to evolve according to an AR(MA)-type process. The latter, referred to as evolution function by Patton (2006), is typically informed by expert opinion. In the absence of expert guidance, nonparametric inference is considered by Hafner and Reznikova (2010), using local likelihood estimation for the time-varying copula dependence parameter in the bivariate case. Other considerations include structural changes and regime-switching models, which allow the form of the copula function to change over time. See Manner and Reznikova (2012) for a survey on time-varying copulas, along with a comparison of several approaches therein.

Due to the notorious difficulty of modeling dependence in higher dimensions, most applications of time-varying (or “dynamic”) copulas have been restricted to bivariate time series. This difficulty in the time-independent (or “static”) setting is addressed by vine copula models (Bedford and Cooke, 2002), which define a multivariate copula sequentially using only unconditional or conditional pair copulas at a time. Several inference techniques (e.g., Aas et al., 2009; Min and Czado, 2010; Hobæk Haff, 2013; Hobæk Haff and Segers, 2015; Nagler and Czado, 2016) and model selection tools (e.g., Dißmann et al., 2013; Min and Czado, 2011; Gruber and Czado, 2015) have been developed for vine copula models in the case of non-temporal multivariate data. These approaches have been also applied to financial time series assuming time-invariant dependence (e.g., Brechmann et al., 2012; Nikoloulopoulos et al., 2012; Brechmann and Czado, 2013). See Aas (2016) for a comprehensive review of vine copula models focusing on their use in financial applications. More recently, modeling strategies to account for time-varying dependence patterns in vine copulas have been investigated in Stöber and Czado (2014) and Fink et al. (2017) via regime switches in the dependence structure, and in So and Yeung (2014) and Almeida et al. (2016) using parametric specifications of the vine copula parameters. However, nonparametric methods to complement these approaches are largely unexplored. One exception is the recent work by Vatter and Nagler (2018), which employs spline smoothing to estimate time-varying dependence in vine copulas.

In this paper, we propose a kernel-based nonparametric method using local likelihood for exploratory analysis of time-varying dependence patterns in multivariate time series. In doing so, we extend (i) the vine copula-GARCH models to incorporate time-varying dependencies in a flexible way, and (ii) the semi-parametric bivariate dynamic copula model in Hafner and Reznikova (2010) to higher dimensions. A significant challenge in this direction concerns the multiplicity of choices the user needs to make in model fitting, in consideration with the associated computational cost. In particular, we address the specification of vine decomposition, selection of a parametric copula family for each pair copula and selection of the tuning parameter for nonparametric smoothing, providing guidance for each of these using simulated data and with an illustrative analysis of multivariate exchange rate dependence. We further discuss the assessment of estimation uncertainty and outline a parametric bootstrap approach to infer dependence dynamics in vine copulas. Compared to the spline-based estimator of Vatter and Nagler (2018), the proposed local likelihood estimator more accurately captures oscillatory and highly nonlinear dependence patterns, at the expense of a higher computational cost.

The outline of the paper is as follows. Section 2 contains a brief description of the multivariate exchange rate data and their marginal models. Section 3 presents time-varying vine copula models and the proposed method of inference. Section 4 reports the results of a simulation study to evaluate the finite-sample performance of the proposed estimator.

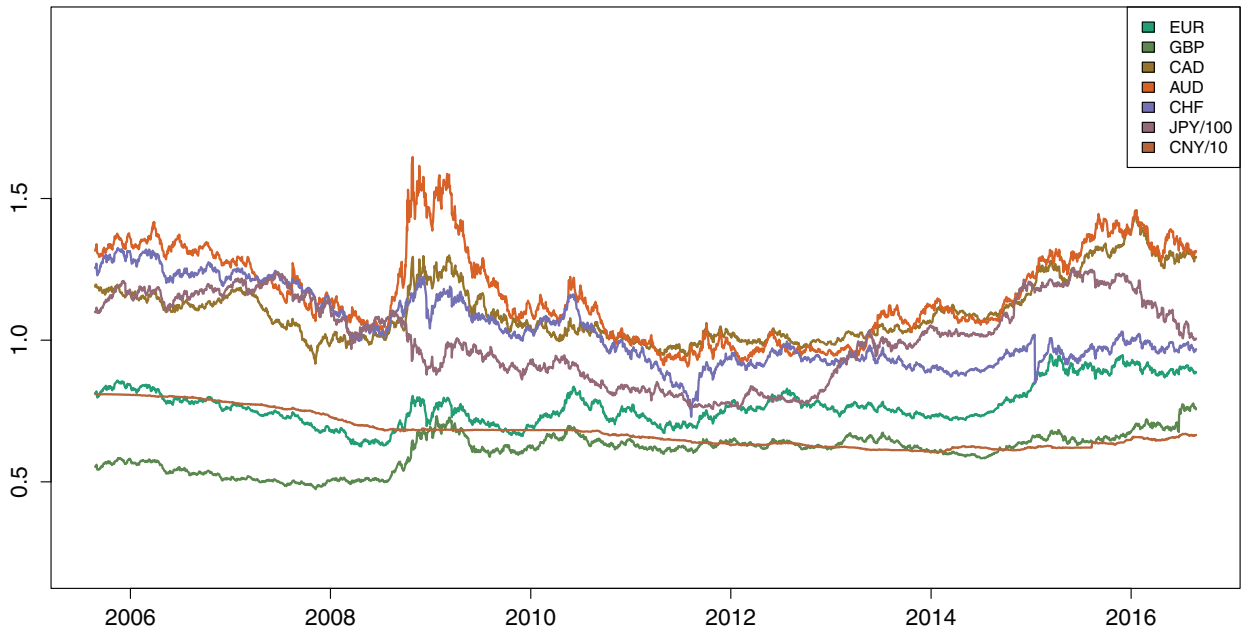


Fig. 1. Daily exchange rates of the seven currencies against USD during the period August 25, 2005–August 25, 2016.

Section 5 revisits the multivariate exchange rate data and provides a guided analysis of temporal dependence patterns. Section 6 concludes with a brief discussion.

2. Exchange rate dependence

Exchange rate dependence has been extensively studied in the copula literature (see Patton, 2006; Hafner and Reznikova, 2010; Dias and Embrechts, 2010; Czado et al., 2012; Stöber and Czado, 2014; Vatter and Nagler, 2018, among others). Here, we consider the daily exchange rates of Euro (EUR), Japanese yen (JPY), Pound sterling (GBP), Australian dollar (AUD), Canadian dollar (CAD), Swiss franc (CHF) and Chinese yuan (CNY) against the U.S. dollar (USD), from August 25, 2005 to August 25, 2016. This period witnessed several financial crises and economic events with regional and global impact. The major ones are the U.S. recession between 2007 and 2009 and the global recession in 2009, followed by the European sovereign debt crisis in late 2009. Other important events include the Brexit referendum on June 23, 2016, the pegging and de-pegging by the Swiss National Bank of CHF against the Euro on Sept 6, 2011 and January 15, 2015, and the devaluation of CNY by the People's Bank of China on August 10–12, 2015.

Our aim is to provide a post hoc evaluation of the impact of these events on the strength of dependence among the exchange rates. A visual check of the daily exchange rates in Fig. 1 indicates clear co-movements among EUR, GBP, CAD, AUD, CHF and JPY. However, the same cannot be said for CNY, which has been tightly controlled under a managed floating exchange rate regime. Nevertheless, we included CNY in our investigations as it has attracted a lot of attention in recent years.

Prior to univariate modeling, we removed 106 dates (public holidays) with a missing value and obtained the exchange rate log-returns defined as $R_t = \log(Y_t/Y_{t-1})$ (see the left column of Fig. 2). Our initial model trials for CNY resulted in very large residuals for the three days of yuan devaluation in August 2015. To prevent the potential negative impact of this misfit on joint modeling, we further removed the log-returns of all exchange rates on August 11–12, 2015. This resulted in 2762 daily log-returns for the analysis. The univariate modeling of the exchange rate log-returns are performed using an AR(1)-GARCH(1,1) model for CNY and AUS, and GARCH(1,1) for the other currencies, all with skewed-t distributed innovations. The parameter estimates for these models, along with the p -values of a weighted Lyung–Box test (Fisher and Gallagher, 2012) (with lag= 10) for the standardized residuals and squared residuals are provided in Table 1.

The standardized residuals $\hat{Z}_{i,t}$ (obtained from the fitted univariate models) and the uniform residuals $\hat{U}_{i,t} = \hat{F}_i^{-1}(\hat{Z}_{i,t})$ are displayed in the middle and right columns of Fig. 2. All currencies except CNY pass the Kolmogorov–Smirnov uniformity test. To safeguard our analysis against model misspecification (especially for CNY), we also used the rank transformation, but observed no significant difference in the results. For brevity of presentation, we focus on the case where the margins are obtained from the parametric innovation distributions, and refer to the corresponding data $\hat{U}_{i,t}$, $i = 1, \dots, 7$, $t = 1, \dots, 2762$, as the copula data.

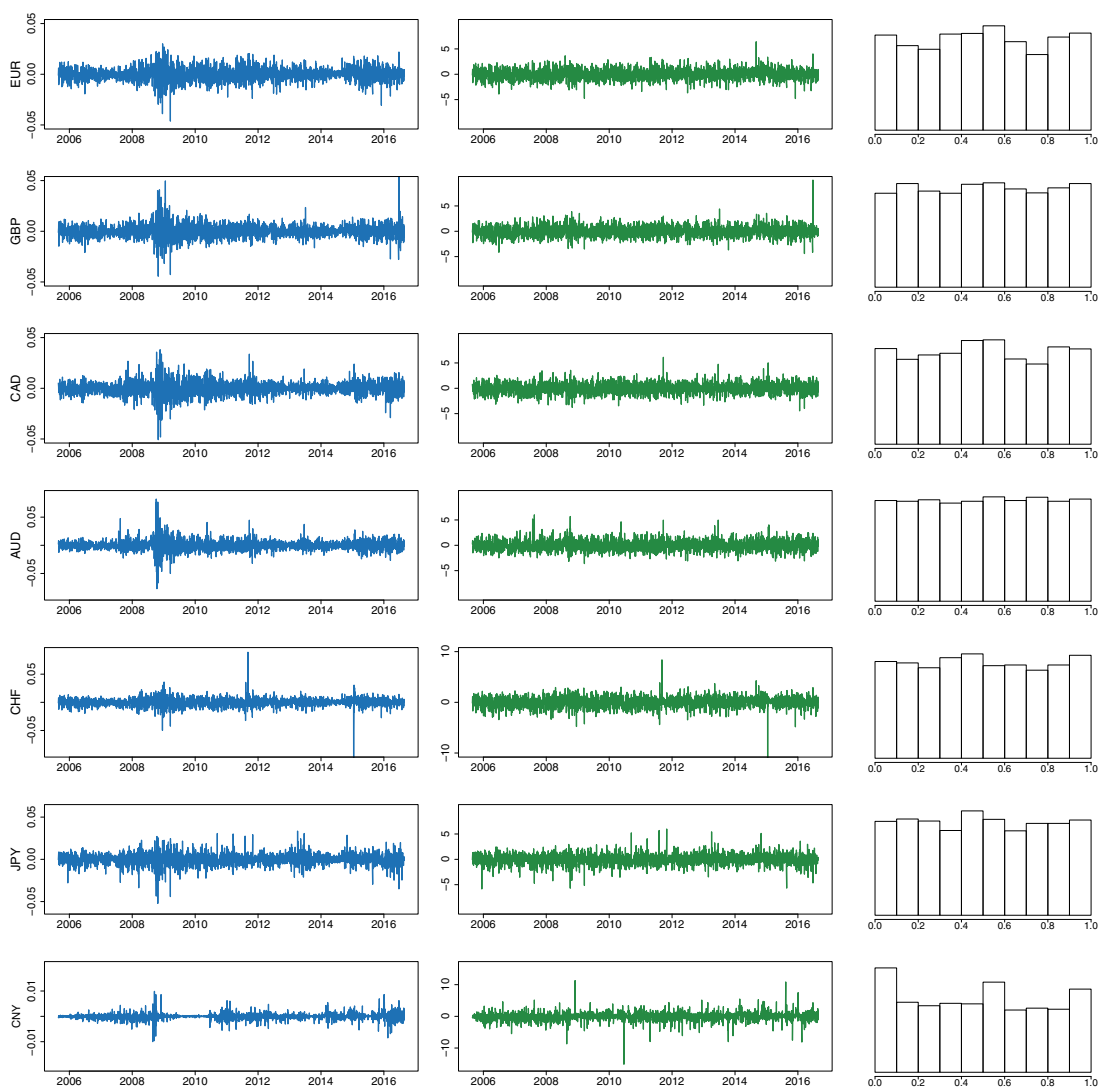


Fig. 2. Time series plots of the log-exchange rate returns (left column) and the standardized residuals (middle column), along with the histograms of the probability integral transformed margins (right column) for the seven currencies.

Table 1

Summary of the univariate GARCH models for the seven currencies.

	EUR	GBP	CAD	AUD	CHF	JPY	CNY
μ	$-1.2e-05$	$3.8e-05$	$4.4e-05$	$-2.3e-06$	$-7.0e-05$	$6.0e-05$	$-2.7e-05$
AR(1)	–	–	–	–0.0453	–0.0907	–	–
ω	$6.5e-08$	$1.0e-07$	$3.4e-07$	$3.2e-07$	$4.3e-07$	$1.6e-09$	
α	0.0354	0.0345	0.0431	0.0509	0.0343	0.0441	0.0778
β	0.9635	0.9631	0.9537	0.9445	0.9580	0.9472	0.8981
Skewness	1.0221	1.0719	1.0256	1.1361	0.9513	0.9712	0.9621
Shape	8.2043	9.2177	8.3726	9.2366	6.1531	5.2959	4.2532
$p_{(WLB)}(z)$	0.9257	0.1439	0.1795	0.2148	0.6984	0.7589	0.3401
$p_{(WLB)}(z^2)$	0.2195	0.5312	0.7908	0.1962	1.0000	0.6713	0.8065

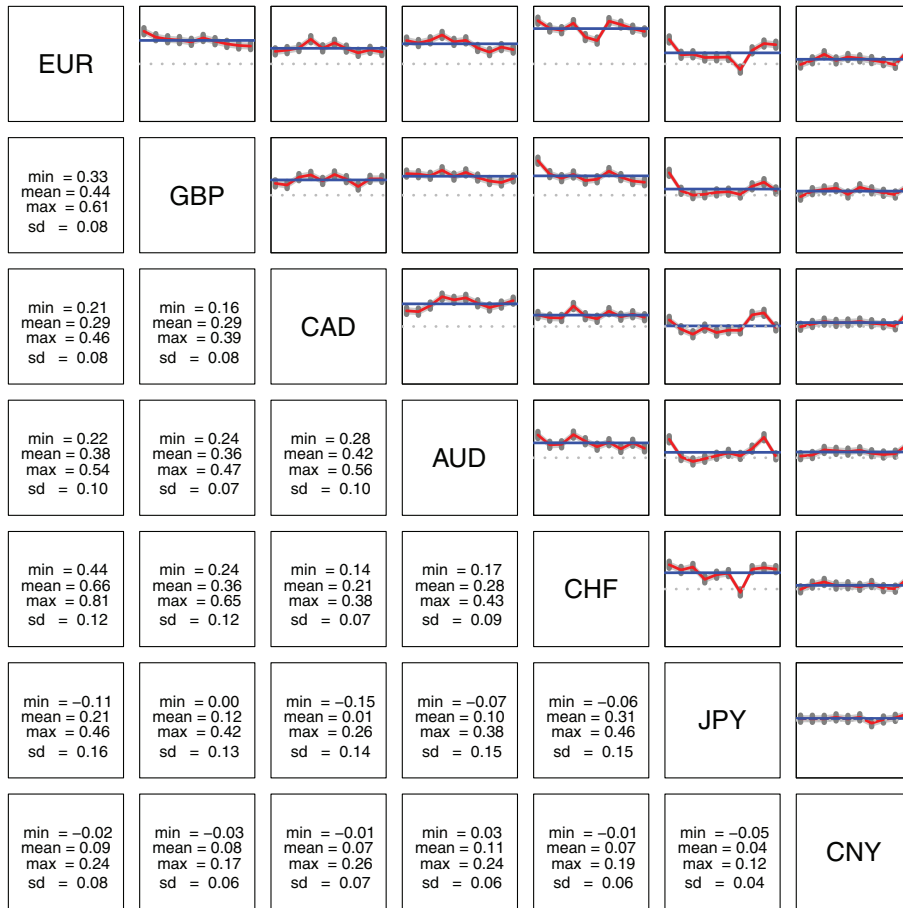


Fig. 3. Descriptive summaries (lower matrix plot) and graphical displays (upper matrix plot) of the empirical Kendall τ estimates over 10 non-overlapping periods (shown in red) along with their large sample confidence intervals (grey bars). The grey dotted line represents $\tau = 0$, while the blue solid line displays the overall (constant) Kendall τ estimates. (For interpretation of the references to color in this figure legend, the reader is referred to the web version of this article.)

As an initial check of time-varying dependence, we calculate the pairwise empirical Kendall τ over 10 non-overlapping periods for each currency pair. The resulting estimates, as well as the large sample confidence intervals for τ at each period, indicate a clear change over time in the strength of dependence among some but not all pairs (see Fig. 3). However, this observation may easily change if one uses a different number of periods or allows the periods to overlap to a certain degree. To provide a formal inference of the time-varying dependencies beyond such initial checks, we take a model-based approach and present dynamic vine copula models in the next section.

3. Dynamic vine copula models

Vine copulas (Bedford and Cooke, 2002; Joe, 1997; Kurowicka and Joe, 2010) are multivariate dependence models, constructed using only unconditional and conditional pair copulas. The construction of vine copulas can be done in many ways, and is typically represented by graphical models, called *vines*.

A regular vine on d variables consists of a nested set of trees $T_i = (N_i, E_i)$ for $i = 1, \dots, d-1$, with N_i and E_i denoting the sets of nodes and edges in tree T_i , respectively. Each edge $e \in E_i$ describes a conditional pair copula $C_{j_e k_e | D_e}$, where the nodes j_e and k_e are conditioned on the set D_e . The multivariate density f of $\mathbf{Z} = (Z_1, \dots, Z_d)$ can then be written as

$$f(\mathbf{z}) = \left[\prod_{i=1}^d f_i(z_i) \right] \times \left[\prod_{i=1}^{d-1} \prod_{e \in E_i} c_{j_e k_e | D_e} \{ F_{j_e | D_e}(z_{j_e} | \mathbf{z}_{D_e}), F_{k_e | D_e}(z_{k_e} | \mathbf{z}_{D_e}); \mathbf{z}_{D_e} \} \right],$$

where f_i denotes the marginal density of Z_i , $F_{i | D_e}$ is its univariate conditional distribution function given the subset \mathbf{z}_{D_e} , and $c_{j_e k_e | D_e}$ is the density of the conditional pair copula associated with the bivariate conditional distribution of Z_{j_e} and Z_{k_e} given the subset \mathbf{z}_{D_e} . In most practical applications of vine copulas, $c_{j_e k_e | D_e}$ is assumed to be independent of the variables in the

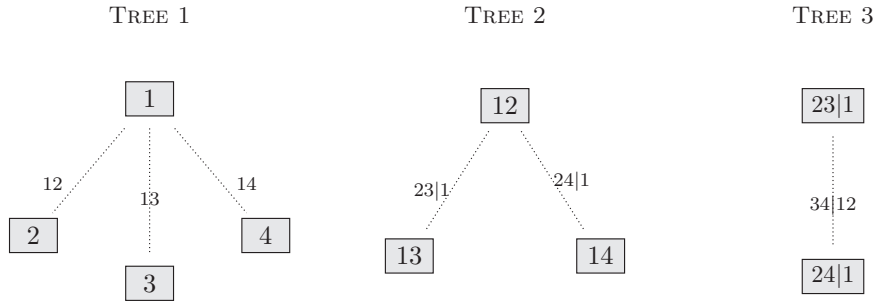


Fig. 4. Tree representation of a regular vine with 4 variables.

conditioning set D_e , leading to the simplification $c_{j_e k_e; D_e}(\cdot, \cdot; \mathbf{z}_{D_e}) = c_{j_e k_e; D_e}(\cdot, \cdot)$. Here, we also make this so-called simplifying assumption. Fig. 4 displays an example of a regular vine in four-dimensions, for which the density factorization is given by

$$f(z_1, z_2, z_3, z_4) = \prod_{i=1}^4 f_i(z_i) \times \prod_{i=2}^4 c_{1i}(F_1(z_1), F_i(z_i)) \prod_{i=3}^4 c_{2i;1}(F_{2|1}(z_2|z_1), F_{i|1}(z_i|z_1)) \\ \times c_{34;12}(F_{3|12}(z_3|z_1, z_2), F_{4|12}(z_4|z_1, z_2)).$$

This vine structure belongs to a special class, called canonical (C-)vine, which has a unique node (key node) at each tree governing the dependence. In four dimensions, all regular vine structures are either C-vines or D-vines, another special class. These two special classes have been very popular in financial applications (Aas, 2016).

Let $U_{i,t} = F_i(Z_{i,t})$, and for an arbitrary bivariate copula $C_{ij}(u, v)$, let $U_{ij;t} = h_{ij}(U_{i,t}, U_{j,t})$ where $h_{ij}(u, v) = \partial C_{ij}(u, v) / \partial v$. Then the regular vine construction for the density c_t of the d -dimensional dynamic copula C_t in (2) is defined as

$$c_t(u_{1,t}, \dots, u_{d,t}) = \prod_{i=1}^{d-1} \prod_{e \in E_i} c_{j_e k_e; D_e, t}(u_{j_e|D_e; t}, u_{k_e|D_e; t}).$$

This amounts to building a vine model using time-varying pair copulas in the first tree and conditioning only in the arguments of time-varying (conditional) pair copulas in the subsequent ones.

When each conditional pair copula belongs to a parametric copula family, the temporal aspects on the dependence structure can be incorporated in the pair copula parameters by allowing them to change over time. For the vine example in Fig. 4, the dynamic copula density takes the parametric form

$$c_t(u_{1,t}, u_{2,t}, u_{3,t}, u_{4,t}) = \prod_{i=2}^4 c_{1i}(u_{1,t}, u_{i,t}; \theta_{1i}(t)) \times \prod_{i=3}^4 c_{2i;1}(u_{2|1;t}, u_{i|1;t}; \theta_{2i;1}(t)) \\ \times c_{34;12}(u_{3|12;t}, u_{4|12;t}; \theta_{34;12}(t)),$$

where the copula parameter functions for conditional pair copulas are denoted by the corresponding subscripts (e.g., $\theta_{34;12}(t)$ represents the copula parameter function of the conditional pair copula $c_{34;12}$). In the case where parametric specifications are appropriate for the copula parameter functions, inference can be achieved using maximum likelihood sequentially for each tree. In the absence of guidance on such parametric forms, a nonparametric strategy to infer time-varying dependence is needed.

3.1. Nonparametric inference for time-varying dependence

Provided that the copula parameter function $\theta(\cdot, t)$ is sufficiently smooth, one can employ nonparametric smoothing techniques to estimate the time-varying dependence in each pair copula of a dynamic vine. Here, we use local likelihood estimation based on kernel smoothing (Hafner and Reznikova, 2010; Acar et al., 2011; Abegaz et al., 2012), but one can also consider spline smoothing (Craiu and Sabeti, 2012; Sabeti et al., 2014; Vatter and Chavez-Demoulin, 2015; Vatter and Nagler, 2018).

Consider first a pair copula $C_{ij|t}$ in the first tree with parameter $\theta_{ij}(t)$. Since the copula parameter has a restricted range for some families, following Acar et al. (2011), we introduce the reparametrization $\theta_{ij}(t) = g^{-1}(\eta_{ij}(t))$, where g^{-1} is an inverse link function that enables unconstrained estimation. Further, to ease the computations, we rescale the time points $t = 1, \dots, T$ using $t^* = t/T$ for $t = 1, \dots, T$. Then, for any t^* in a neighborhood of a fixed t_0^* , we use the linear approximation

$$\eta_{ij}(t^*) \approx \eta_{ij}(t_0^*) + \eta'_{ij}(t_0^*)(t^* - t_0^*) \equiv \eta_0 + \eta_1 (t^* - t_0^*).$$

The parameters η_0 and η_1 are estimated using a kernel-weighted local likelihood function

$$\mathcal{L}(\eta_0, \eta_1, t_0^*, \lambda) = \sum_t^T \log c_{ij} \{u_{i,t}, u_{j,t}; g^{-1}(\eta_0 + \eta_1(t/T - t_0^*))\} K_\lambda(t/T - t_0^*),$$

where λ is a bandwidth and $K_\lambda(\cdot) = \frac{1}{\lambda} K(\cdot/\lambda)$ with a kernel function $K(\cdot)$. The resulting copula parameter estimate at time $t_0 = t_0^* \times T$ is given by $\hat{\theta}(t_0) = g^{-1}(\hat{\eta}_0)$. In practice, one typically considers a grid of fixed points t_0^* in $[0,1]$ to estimate the form of the unknown function. However, in the current setting, the above estimation procedure needs to be repeated for each time point $t = 1, \dots, T$ by letting $t_0 = t$. Once the copula parameter estimates $\hat{\theta}_{ij}(t)$ are obtained, we use $h_{ij}(u, v; \theta) = \partial C_{ij}(u, v; \theta) / \partial v$ to get the pseudo-observations

$$\hat{u}_{i|j,t} = h_{ij}\{u_{i,t}, u_{j,t}; \hat{\theta}_{ij}(t)\}$$

for the next tree. Note that the fitting of each pair copula at Tree k can be done concurrently. However, since the pseudo observations from each pair copula in Tree k are necessary to model the components of Tree $k+1$, one needs to perform estimation following the hierarchy of trees.

3.2. Model selection

Model selection for vine copulas involves the determination of the vine decomposition as well as the selection of copula families for each pair copula component. The current practice is to use the maximum spanning tree algorithm of [Dißmann et al. \(2013\)](#), which is an automated algorithm addressing the vine structure selection by maximizing the empirical Kendall τ at each tree level, and the copula family selection via the Akaike Information Criterion (AIC). Since this algorithm is developed for time-invariant vine copulas, it may not serve well for dynamic vine copula selection. The maximization of the empirical Kendall τ in the Dißmann algorithm advantages the pairs having strong dependencies to appear in the early trees, but would fail to account for time-variation in these dependencies in the current context.

We propose a modification of the Dißmann algorithm for the tree structure selection in vine copulas. Since our interest lies in detecting variations in the dependence patterns over time, we aim to model pair copulas showing a strong overall dependence with high variation in earlier trees. To account for time variation, we specify S (overlapping or non-overlapping) time periods in the range $t = 1, \dots, T$. Then, for each tree level, we calculate the empirical Kendall τ for all possible pairs using the (pseudo-)observations at each period. For regular vines, the vine structure is determined by sequentially selecting a maximum spanning tree via

$$\max_{e_{ij} \in \text{spanning tree}} |\bar{\tau}_{ij}| \times \frac{v_{ij}}{\sum_{(i,j)} v_{ij}},$$

where a spanning tree is a tree on all possible nodes that satisfy the regular vine construction principles (see [Dißmann et al., 2013](#)), $\bar{\tau}_{ij} = S^{-1} \sum_{s=1}^S \tau_{ij,s}$ is the mean empirical Kendall τ over S periods, and $v_{ij} = \max_s |\tau_{ij,s+1} - \tau_{ij,s}|$ quantifies the total variation in Kendall τ over S periods. In the special case of C-vines, the key node i_k of Tree k is sequentially determined using

$$i_k = \max_i \sum_{j \neq i} |\bar{\tau}_{ij}| \times \frac{v_{ij}}{\sum_{(i,j)} v_{ij}}, \quad (i, j) \in \text{Tree } k.$$

Similarly, for D-vines, one can potentially order the variance-weighted mean empirical Kendall τ values over all possible pairs and determine the ordering of nodes in the first tree based on the top $d-1$ pairs.

The selection of copula families of a dynamic vine copula model, on the other hand, requires performing the estimation procedure in [Section 3.1](#) using a set of candidate families for each pair copula component. While the copula families selected by the Dißmann algorithm may provide some guidance, we advise to use copula families that allow both negative and positive dependence, such as Gaussian, t and Frank copulas. Note that copula families are difficult to distinguish when the dependence is moderate-to-weak. Hence, using a copula family that allows for only negative or only positive dependence would fail to capture possible fluctuations between positive and negative values. Our simulation results in [Sections 4.2](#) and [4.5](#) suggest that copula family misspecification does not alter the conclusions on the Kendall τ functions $\tau_{ij}(t)$ in an obvious way. Thus, the choice among Gaussian, t and Frank copulas does not seem to be too critical, and can be conveniently made using AIC under the static vine model. Alternatively, one can employ the cross-validated likelihood criterion outlined in the next section at an increased computational cost.

3.3. Bandwidth selection

The assessment of time variation of the local likelihood approach in [Section 3.1](#) depends heavily on the bandwidth value λ used for estimation. A large λ value yields a global fit with low variance but high bias, whereas a small λ corresponds to an interpolation with low bias but high variance. Hence, the selection of a bandwidth parameter for each pair copula component should be done with care, especially when the aim is to provide an exploratory analysis.

A careful treatment of bandwidth selection typically requires a data-driven approach, e.g., cross-validation based selectors, which can be computationally costly. For dynamic vine copulas, the computational cost drastically increases with the dimension d of the problem at hand and the number of observations T . In the case where interest is, for instance, in weekly, monthly or yearly dependence patterns, one can predetermine the bandwidth parameter for all pair copulas of a dynamic vine accordingly. However, if the interest is exploratory, the computation cost cannot be avoided, but can be strategically reduced. Note that, although appealing, plug-in bandwidth selectors may not approximate well the underlying time variation in the dependencies, as they tend to oversmooth (Loader, 1999). Hence, we employ the cross-validated likelihood criterion of Acar et al. (2011), defined for each pair copula as

$$\lambda_{ij}^* = \operatorname{argmax}_{\lambda \in \Lambda} \sum_{t=1}^T \log c_{ij}\{u_{i,t}, u_{j,t} \mid \hat{\theta}_{ij;\lambda}^{(-t)}(t)\}, \quad (3)$$

where $\hat{\theta}_{ij;\lambda}^{(-t)}(t)$ is obtained by leaving out the observation at time t , and performing local likelihood estimation on the remaining data using the bandwidth value λ . This procedure is followed for all pair copula components separately.

One strategy to reduce computations is to use a shorter time period in bandwidth selection. This approach, however, would be sensitive to the subset choice. Also, a bandwidth selected this way may not be appropriate to reflect the features beyond the selected subset period. An alternative strategy is to use interpolation to approximate the cross-validated likelihood values at large candidate bandwidths. This choice reduces the computational cost by estimating $\hat{\theta}_{ij;\lambda}^{(-t)}(t)$ only at a fine grid of time points. Our investigations indicate that the approximated cross-validated likelihood values are very close to the ones obtained by leave-one-out cross-validation. However, for small bandwidth values, using the latter is a safer choice.

While the cross-validation likelihood criterion is used for model tuning to select a bandwidth, it can also be used to select a copula family among a set of candidate models. That is, the maximization in (3) is performed not only over a set of pilot bandwidth values but also for candidate copula families. However, this comes at an increased computational cost, which, as argued in Section 3.2, can be avoided by selecting a family under the static vine model.

3.4. Uncertainty assessment

Uncertainty assessment in dynamic vine copula models is a challenging task, due not only to the nonparametric nature of the inference procedure, but also to the need for sequential model fitting. The copula data obtained from the assumed innovation distributions, even when the latter are correctly specified, inherit the uncertainty in the fitted GARCH parameters, and carry it over to the inference of pair copula components in the first tree. Consequently, the time-varying dependence parameter estimates at each tree contain additional uncertainty arising from the fitted pair copulas in the previous one, making it difficult to establish asymptotic results for the local likelihood estimator in Section 3.1.

In light of this issue, we propose to estimate uncertainty via parametric bootstrap, with the vine copula structure (tree and families) and the bandwidth value estimates held fixed. The procedure for generating bootstrap samples is summarized in Algorithm 1. For each pair copula, the $(1 - \alpha) \times 100\%$ bootstrap confidence intervals for time-varying dependence are

Algorithm 1 Algorithm for generating bootstrap samples from a dynamic vine-GARCH model.

Given a fitted dynamic vine copula model $C_t(U_{1t}, \dots, U_{dt}; \theta(t))$, and fitted univariate GARCH models G_1, \dots, G_d , repeat the following steps for $b = 1, \dots, B$:

Step 1. For $t = 1, \dots, T$, generate $(U_{1t}^b, \dots, U_{dt}^b)$ from the multivariate copula C_t with the copula parameter vector $\theta(t)$.

Step 2. For $i = 1, \dots, d$, obtain pseudo-innovations $(Z_{1t}^b, \dots, Z_{dt}^b) = (F_i^{-1}(U_{1t}^b), \dots, F_i^{-1}(U_{dt}^b))$, using the inverse probability integral transformation.

Step 3. For $i = 1, \dots, d$, obtain pseudo-data $(Y_{1t}^b, \dots, Y_{dt}^b) = (G_i^{-1}(Z_{1t}^b), \dots, G_i^{-1}(Z_{dt}^b))$, where G_i^{-1} is the GARCH simulator which uses the specification of the fitted model G_i and the pseudo-innovations $(Z_{1t}^b, \dots, Z_{dt}^b)$.

Step 4. Return $(Y_{1t}^b, \dots, Y_{dt}^b)$ for $t = 1, \dots, T$.

constructed using the $(\alpha/2)$ th and $(1 - \alpha/2)$ th quantiles of the bootstrap parameter estimates at each time point.

4. Simulation study

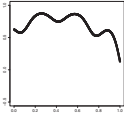
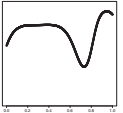
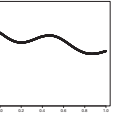
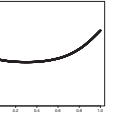
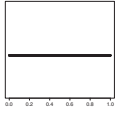
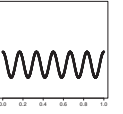
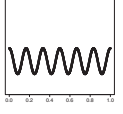
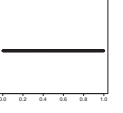
This section reports the results from a simulation study to evaluate the finite-sample performance of the proposed methods. Specifically, we (i) compare the performance of the local likelihood estimator to that of a static vine estimator and that of the spline-based dynamic vine estimator of Vatter and Nagler (2018), (ii) assess the accuracy of the proposed heuristic model selection, (iii) discuss the impact of suggested approximations and model misspecification on the estimation results.

4.1. Simulation setup

We consider two data generating models (DGM) under the vine structure in Fig. 4, with the pair copulas and calibration functions as specified in Table 2. These models share the same first four pair copulas and differ only in the last two compo-

Table 2

Vine models of the examples considered in the simulation study. Reported are the copula families and calibration functions for each pair copula, as well as the graphical representation of the corresponding Kendall tau functions.

Model	Tree 1			Tree 2		Tree 3	
	c_{12}	c_{13}	c_{14}	$c_{23 1}$	$c_{24 1}$	$c_{34 12}$	
DGM 1	(N ; $\eta_1(t)$)	(t ; $\eta_2(t)$)	(C ; $\eta_3(t)$)	(G ; $\eta_4(t)$)	(C ; $\eta_5(t)$)	(F ; $\eta_6(t)$)	
DGM 2					(F ; $\eta_6(t)$)	(C ; $\eta_5(t)$)	
Kendall τ							
							
N=Gaussian, t= $t_{(\nu=4)}$, C=Clayton, G=Gumbel, F=Frank.							
$\eta_1(t) = 2 - 5(t - 0.4)^2 - 0.4 \sin(6\pi t)$, $\eta_2(t) = 0.5 + 3(t - 0.2)^3 + 0.9 \cos(5\pi(t - 0.3)^2)$,							
$\eta_3(t) = 1 - 1.2t - 0.4 \sin(3\pi t)$, $\eta_4(t) = -2 + 5(t - 0.3)^2$, $\eta_5(t) = -1$, $\eta_6(t) = 2 \cos(12\pi t)$.							

nents, $c_{24|1}$ and $c_{34|12}$. The marginal models were specified as GARCH(1,1) with parameters $\omega = 0.001$, $\alpha = 0.050$, $\beta = 0.900$, and the skewed-t distribution with skewness parameter 1 and shape parameter (degrees of freedom) 8. Under each model, we simulated $M = 200$ Monte-Carlo samples of size $n = 1000$.

4.2. Estimation results

For each generated sample, we fit static and dynamic vine models under the true vine structure with correctly specified and selected copula families. Static vine estimates were obtained with the R package *VineCopula* (Schepsmeier et al., 2018), spline-based dynamic vine estimates with the R package *gamCopula* (Nagler and Vatter, 2017), and local likelihood estimates with our own R/ C++ implementation, which is available at <https://github.com/mlsys/LocalCop>. The copula family selection was performed using the Dißmann algorithm based on AIC, which is the default option in the *VineCopula* and *gamCopula* packages. For local likelihood estimation we considered only the Gaussian, t and Frank copulas and selected the family/bandwidth combination yielding the highest cross-validated log-likelihood value. The pilot bandwidth values were set as (0.01, 0.025, 0.05, 0.10, 0.25, 0.5, 1). In cross-validated likelihood calculations we used the leave-one-out method as well as the interpolating approximation outlined in Section 3.3. The results were almost indistinguishable (see Section 4.5 for comparisons).

Fig. 5a and b display the time-varying estimates of Kendall's tau, averaged over $M = 200$ Monte-Carlo samples, from the fitted models under DGM 1 and DGM 2. In the fitted models, bandwidths and families were selected using the cross-validated likelihood criterion with interpolation (between every 20 observations and only for the last four bandwidths). As can be seen, the local likelihood and spline-based estimators are in close agreement and show very similar variability for all pair copula components – except for the case with the calibration function $\eta_6(t)$. There, the spline-based estimator exhibits considerable bias. Similar results were obtained by Vatter and Nagler (2018) for functions with high curvature. We repeated our experiments with $T = 2500$, the sample size in our data application (see Appendix A). While the precision of the estimators increases, the bias in the spline estimator persists for $\eta_6(t)$, in both DGM 1 and DGM 2 settings. In contrast, the local likelihood estimator accurately captures oscillatory and highly nonlinear time-dependence features, even at the smaller sample size $T = 1000$. This, however, comes at a substantially higher computational cost, as local likelihood estimation performs T optimizations for each pair copula, bandwidth parameter, and family combination.

As expected, the static vine model yields an average of the underlying Kendall τ function for each pair copula component, hence fails to identify varying dependence patterns. It is worth mentioning that the default implementation in the *gamCopula* package performs a test to determine whether Kendall's τ can be treated as constant over the given time period or not. In our comparisons, we disabled that feature as more than half of the time the oscillatory function was concluded to be constant under both models, and almost a quarter of the time the corresponding copula was identified as independent.

4.3. Model selection accuracy

We next checked the model selection accuracy of the heuristic approach in Section 3.2. In these assessments, we focused on the selection among canonical vine structures, which amounts to selecting key nodes for the first two trees. Table 3

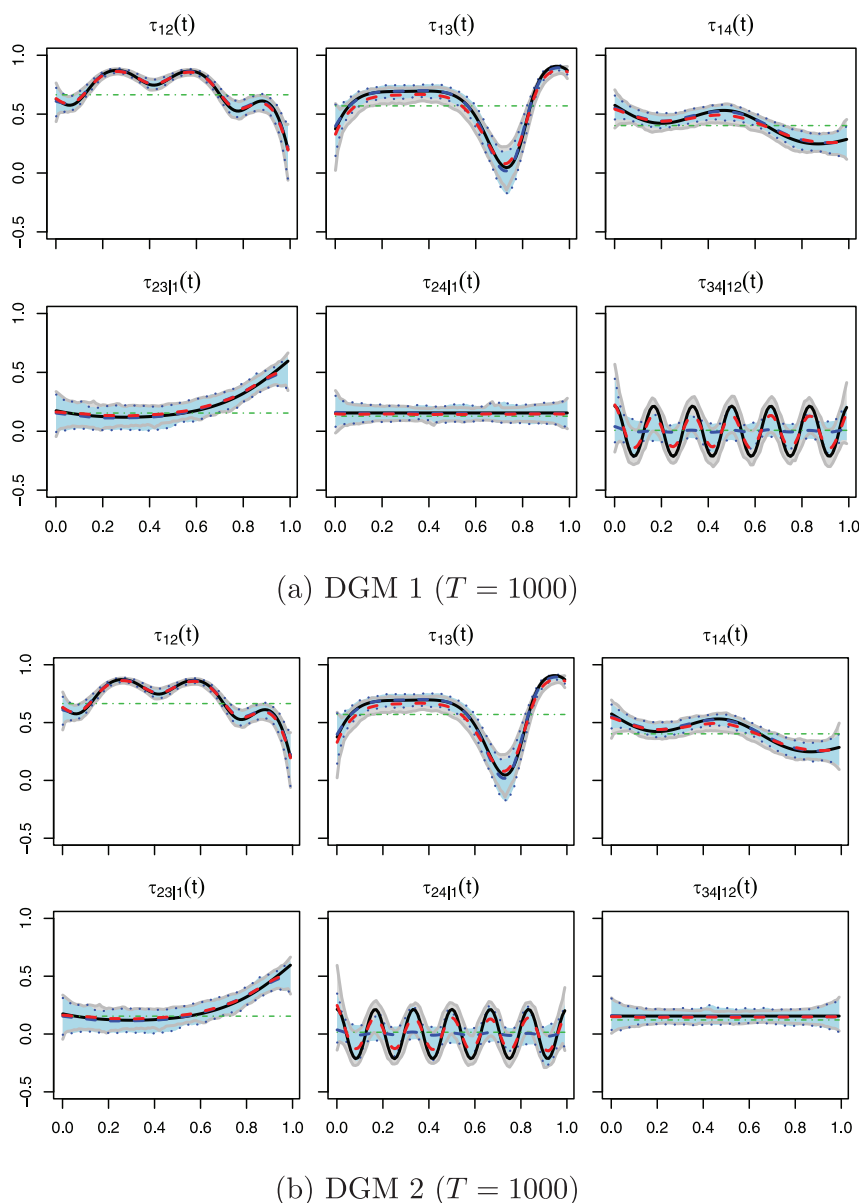


Fig. 5. Average time-varying Kendall τ estimates using the local likelihood estimator (red dashed line) with the 95% Monte-Carlo confidence intervals (grey region) based on $M = 200$ Monte-Carlo samples. The green dot-dashed line displays the average constant Kendall τ estimates, and the blue dashed line represents the average spline estimates along with the 95% Monte-Carlo confidence intervals (blue region). (For interpretation of the references to color in this figure legend, the reader is referred to the web version of this article.)

displays the number of times the heuristic selected the correct model out of 200 datasets of size $n = 1000$ for DGM 1 and DGM 2. Also shown are results from the Dißmann algorithm implemented in the *VineCopula* and *gamCopula* packages. As we can see, the correct vine model was identified with very high accuracy for DGM 1, with slightly better performance with the proposed heuristic than with Dißmann's algorithm. However, both methods fail to identify the correct model in DGM 2, choosing key nodes 1 and 3 instead of 1 and 2 the overwhelming majority of the time.

In light of these two examples, we can conclude that heuristic model selection methods are not well-justified, neither the one proposed here nor the Dißmann algorithm. Hence, vine structure selection remains an open problem.

4.4. Impact of model misspecification

A natural question is whether and how model misspecification affects the reached conclusions on time-varying dependence in dynamic vine copulas. We address this question focusing on DGM 2, where the selected vine structure (in 99% of

Table 3

Number of times correct vine construction was selected out of 200 samples.

	VineCopula	gamCopula	Local Likelihood
DGM 1	171	171	196
DGM 2	0	0	2

the samples) consists of c_{12} , c_{13} , c_{14} , c_{23} ; 1, c_{34} ; 1 and c_{24} ; 13, while the true vine structure has c_{12} , c_{13} , c_{14} , c_{23} ; 1, c_{24} ; 1 and c_{34} ; 12. Since the first four pair copulas are common, potential differences between the two vine structures are likely to be hidden in components that are not explicitly modeled in both.

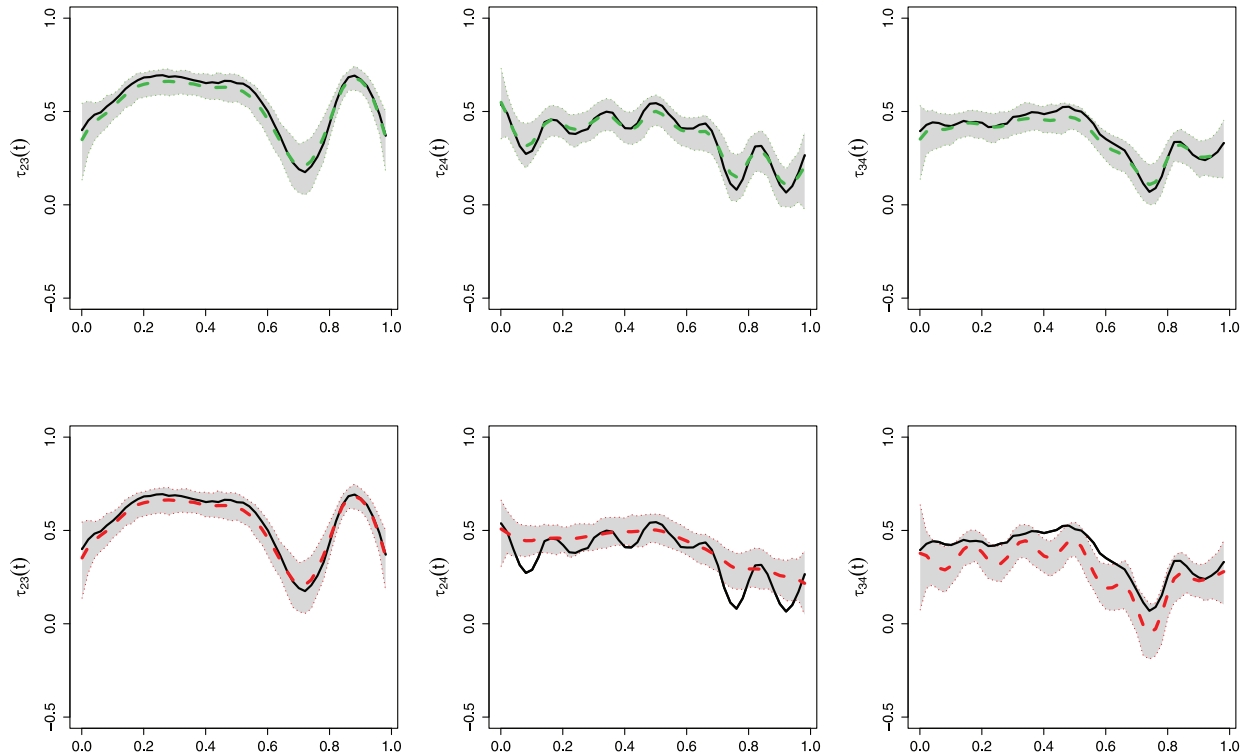


Fig. 6. Unconditional Kendall τ functions under the true data generating model (black solid lines), and the average (dashed lines), 2.5th and 97.5th percentiles (dotted lines) of the unconditional Kendall τ values obtained from the fitted models under the true vine structure (upper panel) and selected vine structure (lower panel).

Here, we evaluate the impact of model misspecification using the unconditional Kendall τ functions, which are obtained via Monte-Carlo integration. Even though these functions are time-varying, the term “unconditional” is used here to emphasize that they quantify the dependence among unconditional pairs. The use of unconditional Kendall τ functions allows for comparison of different vine models in a general and interpretable framework. Fig. 6 displays the unconditional Kendall τ functions which are not explicitly modeled in either vine structures. The black solid lines represent the true Kendall τ functions $\tau_{23}(\cdot)$, $\tau_{24}(\cdot)$ and $\tau_{34}(\cdot)$ under DGM 2. For each generated sample, we obtain the unconditional Kendall τ values from the models fitted under the true and selected vine structures, and display the average, 2.5th and 97.5th percentiles of the unconditional Kendall τ values in the upper (true vine) and lower (selected vine) panels. Under the true vine structure, all Kendall tau functions are accurately estimated. While the true and selected vine structures produce indistinguishable estimates of $\tau_{23}(\cdot)$, they produce inherently different estimates for $\tau_{24}(\cdot)$ and $\tau_{34}(\cdot)$.

4.5. Assessment of approximations

In Section 3, we provided some practical guidance for fitting dynamic vine copulas using local likelihood estimation. Specially, we recommended choosing copula families among the Gaussian, t and Frank copulas, and using interpolation in the cross-validated likelihood calculations for bandwidth and/or family selection. Table 4 reports the integrated mean square error of Kendall τ estimates for each pair copula component under DGM 1 using these approximations. For comparisons, we also report the integrated mean square error of Kendall τ estimates under the static vine model with true copula families

Table 4

Integrated mean square error values of Kendall τ estimates for each pair copula under DGM 1. The estimates were obtained using local likelihood estimation under the true vine construction with (1) true copula families with bandwidth selection without interpolation (2) true copula families with bandwidth selection without interpolation based on interpolation, (3) copula families selected among Gaussian, t and Frank copulas with bandwidth selection without interpolation, (4) copula families selected among Gaussian, t and Frank copulas with bandwidth selection based on interpolation. Also shown are estimates from the static vine model with true copula families and the spline-based dynamic vine model with selected copula families. The last column displays the average computation times in seconds per pair copula.

Fitted model	Tree 1			Tree 2		Tree 3	Average CPU time/pair
	c_{12}	c_{13}	c_{14}	$c_{23; 1}$	$c_{24; 1}$	$c_{34; 12}$	
(1) True families + no interpolation	0.129	0.304	0.154	0.270	0.143	1.208	34.2
(2) True families + interpolation	0.139	0.343	0.141	0.318	0.266	1.433	8.7*
(3) Selected families + no interpolation	0.133	0.361	0.226	0.256	0.157	1.322	90.8
(4) Selected families + interpolation	0.140	0.340	0.209	0.328	0.334	1.640	25.8
Static vine with true families	2.343	5.168	1.062	2.202	0.108	2.780	0.06
Spline-based vine with selected families	0.123	0.231	0.149	0.275	0.157	2.795	1.7

* Average estimation time given a family and bandwidth value is ≈ 2.5 s per pair copula.

and the spline-based dynamic vine model with selected copula families, along with the average computation times of the methods in seconds per pair copula (on an Intel Core i5 with 3.30 GHz CPU and 16 GB RAM). As can be seen, results with and without the interpolating approximation are generally very close, indicating that considerable computational savings can be obtained without much loss of accuracy.

5. Revisiting exchange rates dependence

Upon transforming the seven exchange rate log-returns to copula data using the fitted GARCH models described in Section 2, we fit a canonical vine model by first specifying the key node of Tree 1. This vine structure is chosen as one may expect each currency to have some degree of moderating role on the dependencies among the others. The proposed model selection method, which incorporates both the dependence strength and variation, yields EUR as the key currency. For the specifications of copula families, we consider Gaussian and t-copulas given their $[-1, 1]$ range for Kendall's τ and their popularity in financial applications. The selected families and parameter estimates under the assumption of time-invariant dependence are provided in Table 5. For the t copula, the degrees of freedom parameter is held constant at the estimated value, and only the first parameter is considered as time-varying in local likelihood estimation.

For each pair copula in the vine construction, we consider 9 bandwidth values $\Lambda = \{0.0025, 0.005, 0.01, 0.025, 0.05, 0.10, 0.22, 0.50, 1\}$, corresponding roughly to periods of 1 week, 2 weeks, 1 month, 3 months, 6 months, 1 year, 2.5 years, 5 years and 10 years, respectively. Under the selected families, the cross-validated log-likelihood criterion with interpolation

Table 5

Summary of the time invariant canonical vine copula model with the selected key nodes at each tree for the seven currencies. The selected bandwidth parameters used in local likelihood estimation for each pair copula component are reported in the last column.

Tree	Key node	Pair	Family	θ	df	λ^*
1	EUR	(EUR, GBP)	t	0.635	7.762	0.025
1	EUR	(EUR, CAD)	t	0.446	8.441	0.025
1	EUR	(EUR, AUD)	t	0.557	8.608	0.025
1	EUR	(EUR, CHF)	t	0.854	2.356	0.005
1	EUR	(EUR, JPY)	t	0.311	4.810	0.010
1	EUR	(EUR, CNY)	Gaussian	0.113	–	0.100
2	GBP	(GBP, CAD; EUR)	t	0.219	30.000	0.100
2	GBP	(GBP, AUD; EUR)	t	0.272	27.735	0.100
2	GBP	(GBP, CHF; EUR)	t	0.029	25.295	0.100
2	GBP	(GBP, JPY; EUR)	t	–0.022	13.992	0.100
2	GBP	(GBP, CNY; EUR)	t	0.040	30.000	0.100
3	JPY	(JPY, CAD; EUR, GBP)	t	–0.122	12.388	0.100
3	JPY	(JPY, AUD; EUR, GBP)	t	–0.021	6.427	0.100
3	JPY	(JPY, CHF; EUR, GBP)	t	0.363	14.342	0.100
3	JPY	(JPY, CNY; EUR, GBP)	t	0.031	30.000	0.100
4	CAD	(CAD, AUD; EUR, GBP, JPY)	t	0.442	10.088	0.100
4	CAD	(CAD, CHF; EUR, GBP, JPY)	Gaussian	–0.049	–	0.100
4	CAD	(CAD, CNY; EUR, GBP, JPY)	t	0.035	30.000	0.100
5	AUD	(AUD, CHF; EUR, GBP, JPY, CAD)	t	–0.087	27.242	0.100
5	AUD	(AUD, CNY; EUR, GBP, JPY, CAD)	Gaussian	0.063	–	0.100
6	–	(CHF, CNY; EUR, GBP, JPY, CAD, AUD)	t	0.012	30.000	0.100

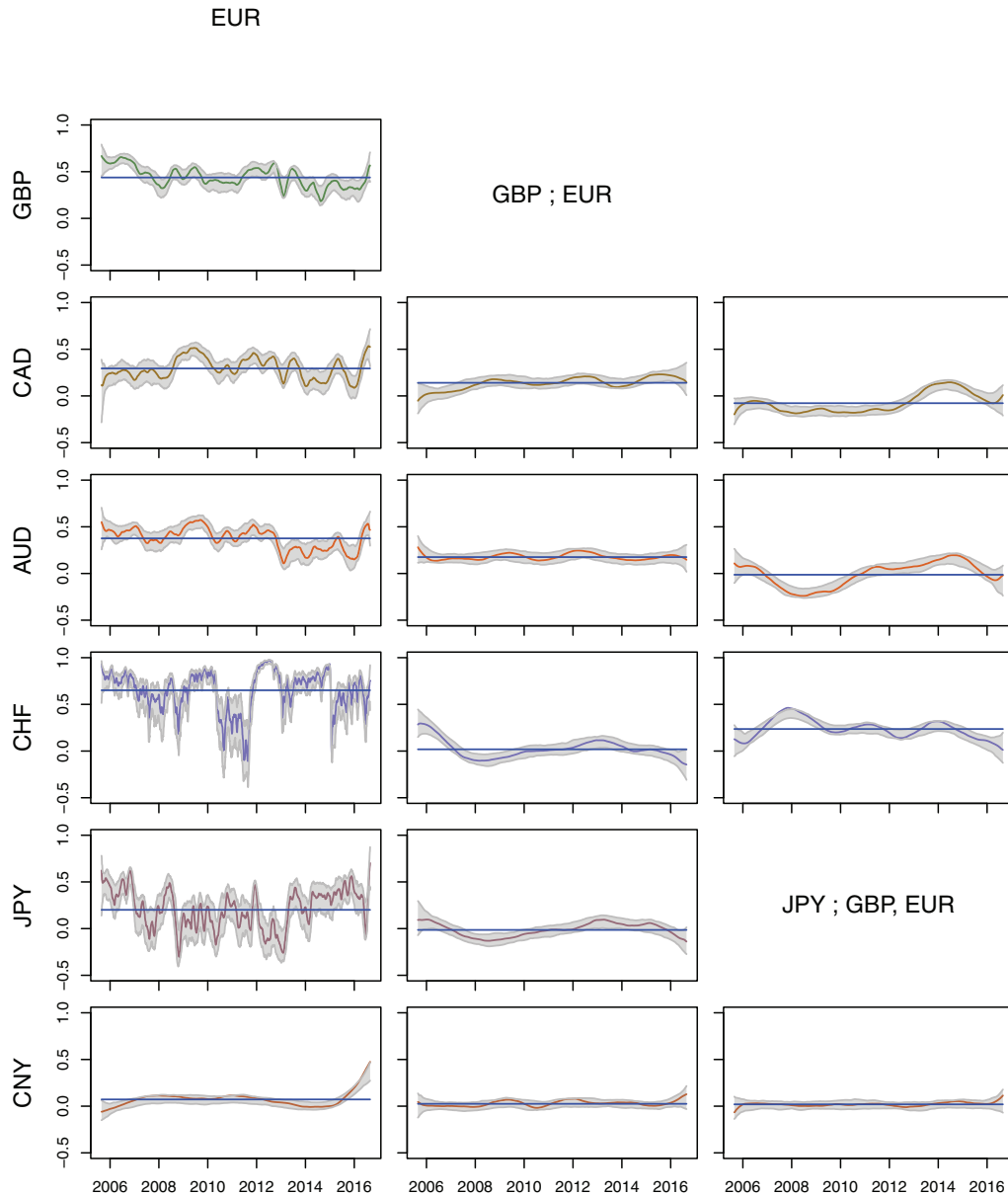


Fig. 7. Time-varying Kendall τ estimates (in various colors) and the 95% bootstrap confidence intervals (in grey) for each pair copula of Tree 1 (left column), Tree 2 (middle column) and Tree 3 (right column), with key nodes EUR, GBP;EUR and JPY; GBP, EUR, respectively. The blue solid line represents the constant Kendall τ estimates. (For interpretation of the references to color in this figure legend, the reader is referred to the web version of this article.)

(between every 20 days, and only for the last five bandwidth values) is used to select a bandwidth parameter. The selected bandwidths for each pair copula are reported in the last column of Table 5. For the pair copulas in Tree 1, we also perform leave-one-out cross validation and obtain the same selected bandwidths as with interpolation.

Using the selected bandwidths, we estimate time-varying copula parameters for each pair copula in Tree 1. The resulting estimates in Kendall's τ scale are displayed in the first column of Fig. 7, along with the 95% bootstrap confidence intervals based on $B = 100$ bootstrap samples. Also shown are the constant Kendall τ estimates obtained assuming time-invariant dependence. After getting the pseudo-data from the fitted time-varying pair copulas in Tree 1, we perform the key node selection, copula family selection, bandwidth selection, and local likelihood estimation in the respective order, and repeat this procedure for each tree. The estimates of time-varying dependencies for Trees 1, 2 and 3 are presented in the columns of Fig. 7, and Trees 4, 5 and 6 in the columns of Fig. 8.

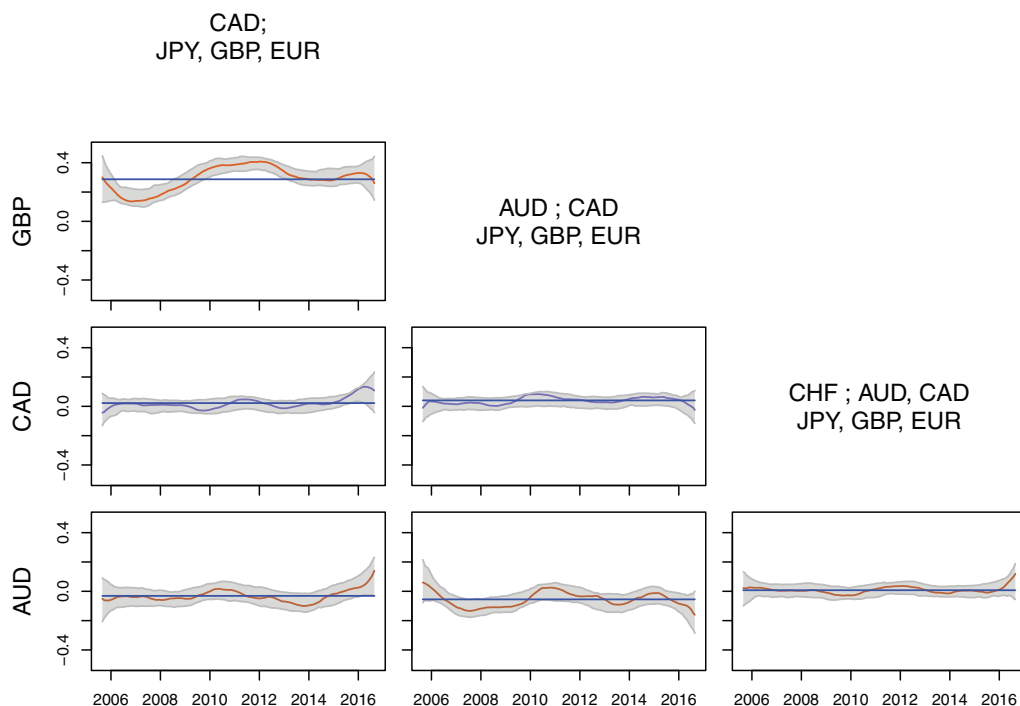


Fig. 8. Time-varying Kendall τ estimates (in various colors) and the 95% bootstrap confidence intervals (in grey) for each pair copula of Tree 4 (left column), Tree 5 (middle column) and Tree 6 (right column), with key nodes CAD; JPY, GBP, EUR and AUD; JPY, GBP, EUR, for the first two, respectively. The blue solid line represents the constant Kendall τ estimates. (For interpretation of the references to color in this figure legend, the reader is referred to the web version of this article.)

Our findings in Tree 1 indicate very similar temporal patterns for GBP, CAD and AUD in terms of the dependence between each of them and EUR over the considered period. In particular, during the global recession, CAD-EUR and AUD-EUR dependence increases significantly, but GBP-EUR only slightly. Around 2013–2014, the dependence between EUR and each of the three aforementioned currencies shows a considerable decrease, which can perhaps be explained by the improvements in economic policy coordination in the Euro Zone. Interestingly, although slight, an increased dependence between EUR and each of the GBP, CAD, and AUD currencies is observed after the Brexit referendum. The dependence between EUR and each of CHF and JPY shows high fluctuations, which follow a similar pattern except during the period 2012–2013. The CHF-EUR dependence is relatively high during the global recession, as well as during the period between the two interventions of the Swiss National Bank. Overall CNY shows weak dependence with other currencies. However, after the yuan devaluation in 2015, its dependence with EUR increases significantly, supporting the integration of CNY into the global economy.

The estimated time-varying dependence patterns in Tree 2 reflect the dependencies between each of the four currencies and GBP after accounting for EUR. While AUD and CNY do not show any significant variation, both CHF and JPY display lower dependence during the global recession period. The dependence between CAD and GBP after accounting for EUR is also considerably lower in 2007. In Tree 3, the dependence between each of CAD, AUD, and CHF with JPY shows significant time-variations, even after accounting for EUR and GBP in the first two trees. In the remaining trees, the dependence patterns indicate almost independence except for the dependence between CAD and AUD in Tree 4. While it is difficult to provide an in-depth explanation for the dependencies at the trees appearing deeper in the hierarchy, the significant time-variations are often observed between currencies that have strong economical and historical ties, such as AUD and CAD. Furthermore, the selected key nodes in the dynamic canonical vine model generally follow the trade volume rankings of these seven currencies.

5.1. Justification of uncertainty assessment

While a theoretical justification of the proposed bootstrap method is difficult to establish, one can use the asymptotic confidence intervals for the semiparametric dynamic copula model in [Hafner and Reznikova \(2010\)](#) to assess the validity of the bootstrap confidence intervals for the unconditional pair copulas in Tree 1. For a given dynamic bivariate copula, the asymptotic $100(1 - \alpha)\%$ confidence interval for the Kendall tau function $\tau(t)$ is constructed pointwise using

$$\hat{\tau}(t) - \hat{B}_{\tau}(t) \pm z_{1-\alpha/2} \hat{V}_{\tau}(t)^{1/2}, \quad (4)$$

where $\hat{B}_{\tau}(t)$ and $\hat{V}_{\tau}(t)$ are stabilized estimates of bias and variance obtained by the delta method ([Hafner and Reznikova, 2010](#)).

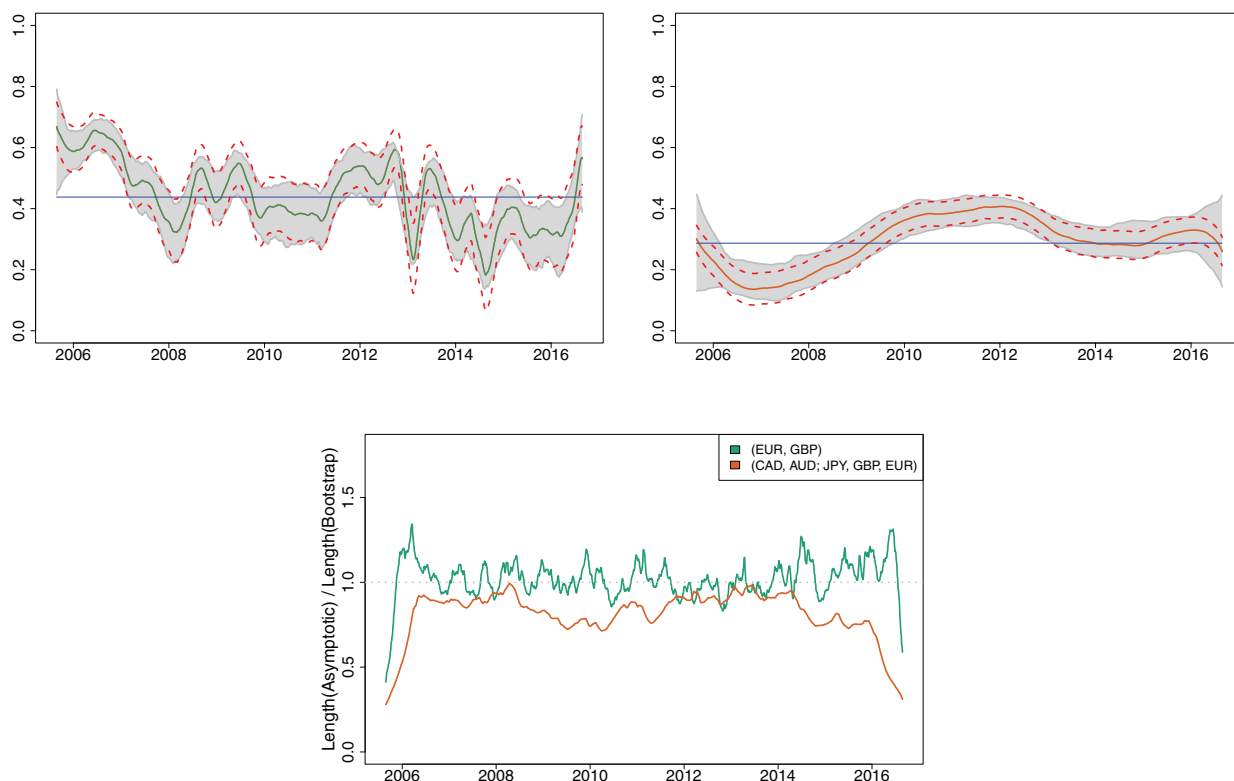


Fig. 9. Comparison of the 95% bootstrap confidence intervals (in grey) and the 95% asymptotic confidence intervals (red dashed lines) for Kendall's τ in the pair copula of (EUR, GBP) in Tree 1 (left) and the pair copula of (CAD, AUD; EUR, GBP, JPY) in Tree 4 (right). The relative lengths of asymptotic and bootstrap confidence intervals are displayed in the bottom row. (For interpretation of the references to color in this figure legend, the reader is referred to the web version of this article.)

As argued in Section 3.4, these asymptotic results hold for unconditional pair copulas, but fail to account for the additional uncertainty in the local likelihood estimation for conditional pair copulas. Hence, one would expect the confidence intervals constructed using (4) to have correct coverage for pair copulas in Tree 1, but suffer from undercoverage for the ones in other trees.

As an illustration, we consider the unconditional pair copula of (EUR, GBP) in Tree 1 and construct the 95% asymptotic confidence intervals for Kendall's tau function as outlined in Hafner and Reznikova (2010). For comparison, we also include the conditional pair copula of (CAD, AUD; EUR, GBP, JPY) in Tree 4 in our investigation.

Fig. 9 displays the asymptotic and bootstrap confidence intervals for Kendall's τ in these pair copulas. The close agreement between the two for the unconditional pair copula suggests that the proposed parametric bootstrap indeed offers a viable approach to infer time-varying dependencies. While the discrepancy between the asymptotic and bootstrap confidence intervals is not too visible for the conditional pair copula, a closer look into the relative lengths of the intervals confirms that the use of asymptotic confidence intervals underestimates the variability in higher order trees and results in uniformly narrower intervals than the proposed bootstrap.

6. Conclusion

This paper presents a nonparametric approach to model multivariate dependence in time series data, using local likelihoods to estimate time-varying dependence patterns in a dynamic vine copula model. Practical aspects concerning the selection of vine structure, copula families, and bandwidth parameters are addressed. A parametric bootstrap method is presented to assess the uncertainty in estimated time-varying dependence parameters. A guided analysis of multivariate exchange rate dependence is provided using data on seven major currencies between 2005–2016. Our findings indicate that significant temporal variations in the dependencies often coincide with the dates of financial crises or other economic events.

A simulation study compares the performance of our method to a recently proposed spline-based estimator for dynamic vine models. Both estimators exhibit similar performance, but the spline estimator sometimes fails to capture oscillatory and other highly nonlinear features. In contrast, the local likelihood estimator with data-driven bandwidth successfully detects such features, but at a sizable increase in computational cost.

The proposed nonparametric approach is mainly for exploratory purposes, having limited forecasting value. However, it can be used to test the assumptions of a parametrically-specified dynamic vine copula model, which if satisfied, suggest that

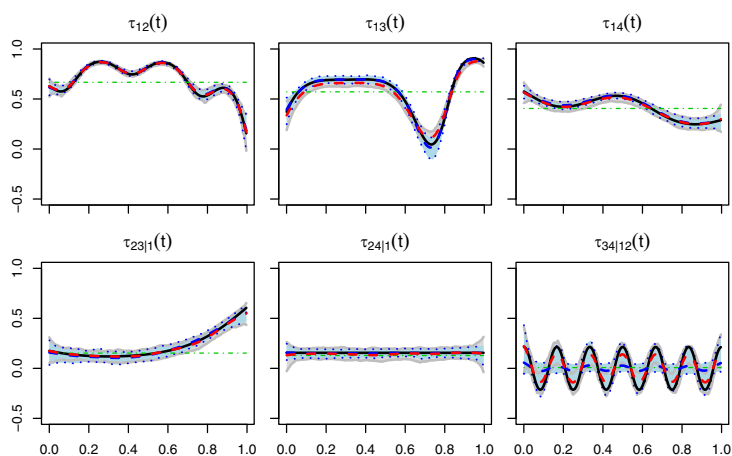
the parametric model could be used in a forecasting context. Another limitation is that the proposed methods are applicable to multivariate time series of the same length and same time scale. The situations where univariate series have different length or are measured at different frequencies involve a number of methodological challenges, and would be the subject of future research. Another research direction is to extend the methods to multivariate spatial or spatio-temporal data using additive models within the local likelihood framework.

Acknowledgements

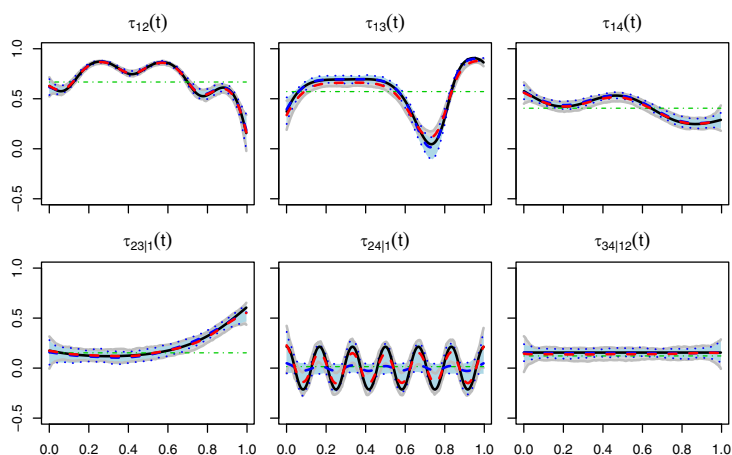
The authors thank the editor, associate editor, and two anonymous referees for their careful review and valuable suggestions. Funding in support of this work was provided by the [Natural Sciences and Engineering Research Council of Canada \(NSERC, RGPIN-2013-435943\)](#), the Canadian Statistical Sciences Institute (CANSSI) Collaborative Research Team Project and the Women for Math Science Program (Technische Universität München) to Acar; by the German Research Foundation (DFG, Project 263890942) to Czado; and by the [Natural Sciences and Engineering Research Council of Canada \(NSERC, RGPIN-2014-04225\)](#) to Lysy.

Appendix A. Additional simulation results

See (Fig. A1).



(a) DGM 1 ($T = 2500$)



(b) DGM 2 ($T = 2500$)

Fig. A1. Average Kendall τ estimates using the local likelihood estimator (red dashed line) with the 95% Monte-Carlo confidence intervals (grey region) based on $M = 200$ Monte-Carlo samples. The green dot-dashed line displays the average constant Kendall τ estimates, and the blue dashed line represents the average spline estimates along with the 95% Monte-Carlo confidence intervals (blue region). (For interpretation of the references to color in this figure legend, the reader is referred to the web version of this article.)

References

- Aas, K., 2016. Pair-copula constructions for financial applications: a review. *Econometrics* 4 (4), 1–15.
- Aas, K., Czado, C., Frigessi, A., Bakken, H., 2009. Pair-copula constructions of multiple dependence. *Insur.: Math. Econ.* 44, 182–198.
- Abegaz, F., Gijbels, I., Veraverbeke, N., 2012. Semiparametric estimation in copula models. *J. Multivar. Anal.* 110, 43–73.
- Acar, E.F., Craiu, R.V., Yao, F., 2011. Dependence calibration in conditional copulas: a nonparametric approach. *Biometrics* 67, 445–453.
- Almeida, C., Czado, C., Manner, H., 2016. Modeling high-dimensional time-varying dependence using dynamic d-vine models. *Appl. Stoch. Models Bus. Ind.* 32 (5), 621–638.
- Bauwens, L., Laurent, S., Rombouts, J.V.K., 2006. Multivariate garch models: a survey. *J. Appl. Econom.* 21 (1), 79–109.
- Bedford, T., Cooke, R.M., 2002. Vines—a new graphical model for dependent random variables. *Ann. Stat.* 30, 1031–1068.
- Bollerslev, T., 1986. Generalized autoregressive conditional heteroskedasticity. *J. Econom.* 31, 307–327.
- Bollerslev, T., 1990. Modelling the coherence in short-run nominal exchange rates: a multivariate generalized arch model. *Rev. Econ. Stat.* 72, 98–505.
- Brechmann, E., Czado, C., 2013. Risk management with high-dimensional vine copulas: an analysis of the euro stoxx 50. *Stat. Risk Model.* 30 (4), 307–342.
- Brechmann, E., Czado, C., Aas, K., 2012. Truncated regular vines in high dimensions with application to financial data. *Can. J. Stat.* 40, 68–85.
- Chen, X., Fan, Y., 2006. Estimation and model selection of semiparametric copula-based multivariate dynamic models under copula misspecification. *J. Econom.* 135 (1–2), 125–154.
- Cherubini, U., Luciano, E., Vecchiato, W., 2004. *Copula Methods in Finance*. John Wiley & Sons, Hoboken, NJ.
- Craiu, R.V., Sabetti, A., 2012. In mixed company: Bayesian inference for bivariate conditional copula models with discrete and continuous outcomes. *J. Multivar. Anal.* 110, 106–120.
- Czado, C., Schepsmeier, U., Min, A., 2012. Maximum likelihood estimation of mixed c-vines with application to exchange rates. *Stat. Model.* 12 (3), 229–255.
- Dias, A., Embrechts, P., 2010. Modeling exchange rate dependence at different time horizons. *J. Int. Money Financ.* 29 (8), 1687–1705.
- Dißmann, J., Brechmann, E., Czado, C., Kurowicka, D., 2013. Selecting and estimating regular vine copulae and application to financial returns. *Comput. Stat. Data Anal.* 59, 52–69.
- Engle, R.F., 2002. Dynamic conditional correlation: a simple class of multivariate generalized autoregressive conditional heteroskedasticity models. *J. Bus. Econ. Stat.* 20 (3), 339–350.
- Engle, R.F., Bollerslev, T., 1986. Modelling the persistence of conditional variances. *Econom. Rev.* 5 (1), 1–50.
- Fink, H., Klimova, Y., Czado, C., Stöber, J., 2017. Regime switching vine copula models for global equity and volatility indices. *Econometrics* 5 (1).
- Fisher, T., Gallagher, C., 2012. New weighted portmanteau statistics for time series goodness-of-fit testing. *J. Am. Stat. Assoc.* 107 (498), 777–787.
- Van den Goorbergh, R., Genest, C., Werker, B.J.M., 2005. Bivariate option pricing using dynamic copula models. *Insur.: Math. Econ.* 37, 101–114.
- Gruber, L., Czado, C., 2015. Sequential bayesian model selection of regular vine copulas. *Bayesian Anal.* 10, 937–963.
- Hafner, C., Reznikova, O., 2010. Efficient estimation of a semiparametric dynamic copula model. *Comput. Stat. Data Anal.* 54 (11), 2609–2627.
- Hobæk Haff, I., 2013. Parameter estimation for pair-copula constructions. *Bernoulli* 19, 462–491.
- Hobæk Haff, I., Segers, J., 2015. Nonparametric estimation of pair-copula constructions with the empirical pair-copula. *Comput. Stat. Data Anal.* 84, 1–13.
- Joe, H., 1997. *Multivariate Models and Dependence Concepts*. Chapman & Hall, London.
- Joe, H., 2014. *Dependence Modeling with Copulas*. Chapman & Hall.
- Jondeau, E., Rockinger, M., 2006. The Copula-GARCH model of conditional dependencies: an international stock market application. *J. Int. Money Financ.* 25, 827–853.
- Kurowicka, D., Joe, H. (Eds.), 2010. *Dependence Modeling: Handbook on Vine Copulae*. World Scientific Publishing, Singapore/SG.
- Loader, C., 1999. Bandwidth selection: classical or plug-in? *Ann. Stat.* 27 (2), 415–438.
- Manner, H., Reznikova, O., 2012. A survey on time-varying copulas: specifications, simulations and application. *Econom. Rev.* 31 (6), 654–687.
- McNeil, A.J., Frey, R., Embrechts, P., 2005. *Quantitative Risk Management: Concepts, Techniques and Tools*. Princeton University Press, Princeton, NJ.
- Min, A., Czado, C., 2010. Bayesian inference for multivariate copulas using pair-copula constructions. *J. Financ. Econom.* 8 (4), 511–546.
- Min, A., Czado, C., 2011. Bayesian model selection for multivariate copulas using pair-copula constructions. *Can. J. Stat.* 39 (2), 239–258.
- Nagler, T., Czado, C., 2016. Evading the curse of dimensionality in nonparametric density estimation with simplified vine copulas. *J. Multivar. Anal.* 151, 69–89.
- Nagler, T., Vatter, T., 2017. *Gamcopula: Generalized Additive Models for Bivariate Conditional Dependence Structures and Vine Copulas*. R package version 0.0-4.
- Nelsen, R.B., 2006. *An Introduction to Copulas*, 2nd ed. Springer, New York.
- Nikoloulopoulos, A., Joe, H., Haijun, L., 2012. Vine copulas with asymmetric tail dependence and applications to financial return data. *Comput. Stat. Data Anal.* 56 (11), 3659–3673.
- Patton, A.J., 2006. Modelling asymmetric exchange rate dependence. *Int. Econ. Rev.* 47, 527–556.
- Patton, A.J., 2012. A review of copula models for economic time series. *J. Multivar. Anal.* 110, 4–18.
- Sabetti, A., Wei, M., Craiu, R., 2014. Additive models for conditional copulas. *Stat* 3 (1), 300–312.
- Schepsmeier, U., Stoeber, J., Brechmann, E. C., Graeler, B., Nagler, T., Erhardt, T., 2018. *Vinecopula: Statistical Inference of Vine Copulas*. R package version 2.1-8.
- Sklar, A., 1959. Fonctions de répartition à n Dimensions et Leurs Marges, 8. Publications de l'Institut de statistique de l'Université de Paris, pp. 229–231.
- So, M., Yeung, C., 2014. Vine-copula garch model with dynamic conditional dependence. *Comput. Stat. Data Anal.* 76, 655–671.
- Stöber, J., Czado, C., 2014. Regime switches in the dependence structure of multidimensional financial data. *Comput. Stat. Data Anal.* 76, 672–686.
- Tse, Y.K., Tsui, A.K.C., 2002. A multivariate generalized autoregressive conditional heteroscedasticity model with time-varying correlations. *J. Bus. Econ. Stat.* 20 (3), 351–362.
- Vatter, T., Chavez-Demoulin, V., 2015. Generalized additive models for conditional dependence structures. *J. Multivar. Anal.* 141, 147–167.
- Vatter, T., Nagler, T., 2018. Generalized additive models for pair-copula constructions. *J. Comput. Graph. Stat.* 27 (4), 715–727. doi:10.1080/10618600.2018.1451338.